

Lepton Spectra from $e^+e^- \rightarrow W^+W^-$ in the BESS model

P. Poulose^{1,*}, S. D. Rindani^{2,†} and L. M. Sehgal^{3,‡}

¹*Institute of Theoretical Physics E, RWTH Aachen,
D-52056 Aachen, Germany*

²*Theory Group, Physical Research Laboratory,
Navrangpura, Ahmedabad-380 009, India*

November 2, 2018

Abstract

We investigate the reaction $e^+e^- \rightarrow W^+W^-$, $W^- \rightarrow l^-\bar{\nu}$ in a strong coupling scenario as implemented in the BESS model. Energy and angle spectra of the secondary lepton are calculated and compared with the predictions of the Standard Model. These spectra provide a determination of the fraction f_0 of longitudinally polarized W 's, and the backward fraction of secondary leptons, f_{back} . Assuming BESS parameters allowed by present data, we give numerical estimates of the effects to be expected at an e^+e^- collider of energy $\sqrt{s} = 500 - 800$ GeV.

1 Introduction

Since its introduction about three decades ago the Standard Model (SM) has undergone stringent experimental tests, which it has so far been able to face successfully. At the same time an important area of the theory is yet to be tested. This is the mechanism that generates particle masses in the SM, namely the Higgs mechanism. The idea of a scalar field which acquires a non-zero vacuum expectation value is the central concept of the Higgs mechanism. This has the consequence of a physical scalar particle, the mass of which the theory is unable to predict. Indirect mass bounds obtained from high precision measurements at LEP and SLC are drawn with the assumption that this particle is elementary and sufficiently light.

An alternative scenario that has been discussed in the literature is the so-called “heavy-Higgs” limit [1]. The SM relation $m_H^2 = \lambda v^2$ between the Higgs mass, m_H and the electroweak scale, v , holds so long as λ , the quartic coupling of the scalar

*poulos@physik.rwth-aachen.de

†saurabh@prl.ernet.in

‡sehgal@physik.rwth-aachen.de

fields is perturbatively small. In the limit of large λ , the Goldstone bosons of the scalar sector become strongly interacting, manifesting themselves as strongly interacting gauge bosons. The elementary Higgs particle disappears from the spectrum, and instead various composite states appear as resonances in the WW channel. A specific approach in this direction goes under the name of BESS (Breaking Electroweak Symmetry Strongly). Reference [2] gives a list of papers in this context. In essence, BESS borrows the idea of hidden local symmetry [3] of the non-linear σ -model, which has been applied with success to the understanding of pion-pion interactions at low energies [4]. By analogy with the pion-pion system, it is conjectured that there is a ρ -like resonance (gauge boson of the hidden local symmetry) in the electroweak interactions, which couples strongly to WW pairs. The mass of the new gauge boson, m_V , the gauge coupling of the new gauge sector, g'' , and its direct fermionic coupling, b , are the parameters of the BESS model in addition to the parameters of the SM. A possible guideline for the parameter g'' is the analogous coupling $2 g_{\rho\pi\pi} \sim 2 \sqrt{12} \pi \sim 12$ in the ρ - π - π system. A simple scaling of the ρ resonance mass, m_ρ to the electroweak scale sets the typical mass of the new resonance. This gives

$$m_V = \frac{f_\pi}{v} m_\rho \sim 2 \text{ TeV}$$

where f_π is the pion decay constant. Due to mixing of the standard gauge sector with the hidden gauge sector, the new gauge bosons have induced coupling to the fermions even in the absence of the direct fermionic coupling, b . Mixing also influences the couplings of the standard gauge particles, the Z and the W 's, to the fermions and among themselves. A detailed description of the model can be found in the first two references in [2].

Precision measurements done at the LEP and SLC colliders restrict the parameter space of the BESS model. From the measured value of the radiative correction parameter ϵ_3 [5], Casalbuoni, *et al*, [6] obtained constraints in the $(g/g'', b)$ space. Here g is the standard weak coupling. BESS contribution to ϵ_3 is given in terms of the parameters as

$$\epsilon_3^{\text{BESS}} = -b + \left(\frac{g}{g''} \right)^2.$$

Considering this along with the SM corrections (obtained with the Higgs mass treated as a cut off) gives an allowed region of parameter space, defined by [6]

$$-\left(4.6_{+0.5}^{-1.0}\right) \times 10^{-3} \leq \epsilon_3^{\text{BESS}} \leq \left(-0.5_{-0.5}^{+1.0}\right) \times 10^{-3}.$$

One can also consider the implications of the recent LEP2 data on the cross section of WW pair production in the energy range of 183-207 GeV. These results agree with the SM prediction to an accuracy of about 2% [7]. Our analysis shows that at c.m. energies around 200 GeV, the sensitivity of the cross section to g/g'' is negligible as long as its value is less than about 0.1. This enables us to put an upper limit of 0.01 on the value of b . Combining this with the constraint from ϵ_3 restricts the value of g/g'' to be less than 0.05. We will accordingly consider parameter values in the general domain $0 \leq b \leq 0.01$ and $0 \leq (g/g'') \leq 0.05$.

The question of phenomenological interest is how these new gauge bosons influence experimental observables. For example, the neutral gauge boson of the new gauge

sector (V^0) behaves very much like the familiar Z boson, interacting with different neutral currents. This can influence processes like $e^+e^- \rightarrow f\bar{f}$ or $e^+e^- \rightarrow W^+W^-$. Due to the comparatively strong coupling of the new gauge boson with W , pair production of W in electron-positron collisions is a suitable candidate for testing the BESS model. Leptonic linear colliders at high energies starting from 500 GeV are expected to be operational in the foreseeable future. Previous studies [8] emphasise that the sensitivity to new physics is enhanced if one looks at the polarization of W . One way to do this is to look at the lepton spectra in $e^+e^- \rightarrow W^+W^-$ with $W^- \rightarrow l^-\bar{\nu}$. We will calculate the correlation of the lepton energy and the lepton angle (in the lab frame), following the analysis of Koval'chuk *et al.* [9]. The energy spectrum turns out to be a function of the diagonal elements of the W^- spin density matrix (f_0 , f_+ and f_-), while the angular distribution contains additional information involving also the non-diagonal elements.

In the next section we give expressions for the cross section and the details of the observables considered. In Sec. 3 we discuss the results, and make some concluding remarks in Sec. 4.

2 Signals from $e^+e^- \rightarrow W^+W^-$

To study the strongly interacting W 's in the context of the BESS model we consider the process $e^+e^- \rightarrow W^+W^-$. In addition to the SM channels, this process gets contribution from an s -channel exchange of the new gauge boson, V^0 (Fig.1).

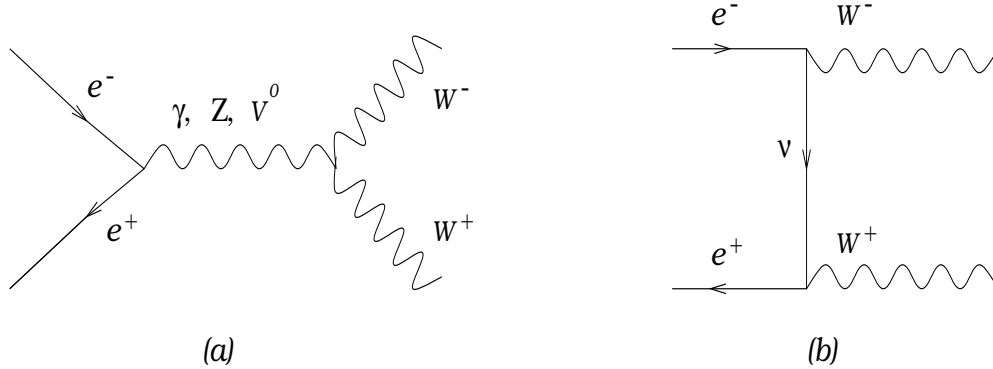


Figure 1: Feynman diagrams contributing to the process $e^+e^- \rightarrow W^+W^-$.

The relevant fermionic and gauge couplings are given in the Appendix. The energy-angle correlation of the secondary lepton is calculated following the procedure of Ref. [9], using a Breit-Wigner form for the W^- propagator:

$$\frac{d\sigma}{dx d\cos\theta_l} = \frac{3}{2} \frac{\alpha^2}{s} \text{BR}(W^- \rightarrow e^-\bar{\nu}) A(s, x, \theta_l) \times \left[\tan^{-1}\left(\frac{m_W}{\Gamma_W}\right) + \tan^{-1}\left(\frac{sx}{m_W\Gamma_W} - \frac{s\tau}{m_W\Gamma_W(1-x)}\right) \right], \quad (1)$$

where

$$A(s, x, \theta_l) = C_s A_s + C'_s A'_s + C_{int} A_{int} + C_t A_t,$$

with

$$\begin{aligned}
A_s &= -\frac{3}{2} - \tau - \frac{\tau}{x} + \frac{\tau^2}{x^2} + \frac{x}{\tau}(1-x) \left(1 + \frac{1}{4\tau}\right) + \\
&\quad \left(-\frac{5}{2} - \tau + 3\frac{\tau}{x} - 3\frac{\tau^2}{x^2} + \frac{1}{2\tau} + \frac{x}{\tau}(1-x) \left(1 - \frac{1}{4\tau}\right)\right) \cos^2 \theta_l \\
A'_s &= 2 \left(1 + \frac{1}{4\tau} - 2x - 2\frac{\tau}{x}\right) \cos \theta_l \\
A_{int} &= -2\tau + \frac{x}{\tau} - 2 + \frac{x}{2\tau}(1-x) \left(1 + \frac{1}{2\tau}\right) + \\
&\quad \left(1 + \frac{1}{2\tau} - \frac{2\tau}{x} - 2x\right) \cos \theta_l - \left(1 - \frac{1}{2\tau}\right) \left(1 - \frac{x(1-x)}{2\tau}\right) \cos^2 \theta_l - \\
&\quad R x^2 \left(2 + (\cos \theta_l - \beta \cos \theta) \left(2 - \left(1 + \frac{1}{\tau}\right) \beta \cos \theta + \cos \theta_l\right)\right) \\
A_t &= \left(-2 + \frac{2x}{\tau} + \frac{x(1-x)}{4\tau^2}\right) + \frac{\cos \theta_l}{2\tau} + \left(1 - (1-x)\frac{x}{2\tau}\right) \frac{\cos^2 \theta_l}{2\tau} - \\
&\quad \frac{2}{\tau} x^2 R (\beta \cos \theta - \cos \theta_l) \beta \cos \theta + 2x^2 a R^3 (\beta \cos \theta - \cos \theta_l)^2.
\end{aligned}$$

Here $x = \frac{2E_l}{\sqrt{s}}$, where E_l is the energy of the secondary lepton in the e^+e^- c.m. frame, \sqrt{s} being the collider energy; $\tau = \frac{m_W^2}{s}$; $a = 2\tau - 1 + \beta \cos \theta \cos \theta_l$, where $\cos \theta = \frac{1}{\beta}(1 - \frac{2\tau}{x})$ is the scattering angle of W^- , $\beta = \sqrt{1 - \frac{4m_W^2}{s}}$ is the velocity of W^- , and $\cos \theta_l$ is the polar angle of the secondary lepton, all in the c.m. frame; and $R^{-2} = 4\tau^2 + (\beta \cos \theta - \cos \theta_l)(\beta \cos \theta - \beta^2 \cos \theta_l)$. $\text{BR}(W^- \rightarrow e^- \bar{\nu})$ is the leptonic branching ratio of W^- . The coefficients, C_s , C'_s , C_t and C_{int} involve various couplings, and are given in the Appendix.

This formula gives the correlation of secondary lepton angle and energy. The energy spectrum, integrated over all $\cos \theta_l$ is equivalent to the angular distribution of the lepton in the rest frame of the W^- :

$$\frac{1}{\sigma} \frac{d\sigma}{d \cos \theta^*} = \frac{3}{4} f_0 \sin^2 \theta^* + \frac{3}{8} f_+ (1 - \cos \theta^*)^2 + \frac{3}{8} f_- (1 + \cos \theta^*)^2, \quad (2)$$

by virtue of the kinematical relation [12]

$$E_l = \frac{\sqrt{s}}{4} (1 - \beta \cos \theta^*).$$

Here θ^* is the polar angle of the lepton in the rest frame of the W with z axis along the boost direction. f_0 gives the fractional cross section of the longitudinal W^- , while f_{\pm} give that of the positive and negative helicity W^- 's. LEP2 has been able to measure the longitudinal fraction, f_0 with an accuracy of 5% [10]. Although this does not restrict the parameters of the BESS model better than the total cross section measurements at LEP2, the measurement of f_0 is of prime importance in the search for new physics at high energies.

The energy distribution is studied in the context of BESS by Werthenbach and Sehgal in [11]. One advantage of the energy-angle correlation given in Eq. 1 is that it enables us to study the effect of angular cuts, due to geometrical acceptance. For

example an angular cut of 10° , as expected in the case of TESLA, distorts the energy spectrum in a way that can be computed using Eq. 1.

From the angular distribution of the lepton one can obtain, in particular, the backward fraction. Since the t -channel ν -exchange contribution peaks in the forward direction, we expect the BESS-SM difference to be more pronounced in the backward hemisphere. At high energies, the leptons are emitted more or less collinearly with the W . Therefore the backward fraction of the leptons is expected to be a suitable observable to distinguish BESS from SM.

These correlations and distributions can be used to obtain limits on the BESS parameters that can be probed at future colliders. The secondary spectra, when combined with the primary observables studied in Ref. [8], could help pin down the parameter space better. Our aim in this paper is to consider typical parameter values allowed by present experiments, and study deviations expected at a collider running at different c.m. energies.

We summarise the results of our analysis in the next section.

3 Results

In our numerical analysis we consider the couplings restricted to $0 \leq b \leq 0.01$ and $0.01 \leq (g/g'') \leq 0.05$. Mass of the new resonance is expected to be in the TeV range, as suggested by the ρ -resonance mass in hadron-physics. We find that the observables are not very sensitive to the location of the resonance except rather close to the resonance. We give results for a 1 TeV resonance (which has a width $\Gamma_V \sim 12$ GeV) and also for $m_V = 2$ TeV (in which case $\Gamma_V \sim 350$ GeV). Our results are presented for two possible c.m. energies, 500 GeV and 800 GeV as envisaged, e.g., for TESLA.

3.1 Total Cross section:

In Fig 2 we recapitulate $\sigma(e^+e^- \rightarrow W^+W^-)$ in the SM and in the BESS scenario. Important feature is that the cross sections differ significantly only in the vicinity of the resonance. Numerical values for different choices of $(m_V, g/g'', b)$ as well as electron polarization are given in Table 2.

3.2 Energy Spectrum of the Secondary Lepton:

The expression for energy distribution in terms of the polarization fractions, as obtained from Eq. 2, is

$$\frac{1}{\sigma} \frac{d\sigma}{dx} = \frac{2}{\beta^3} \left\{ \frac{3}{4} f_0 \left(\beta^2 - (1 - 2x)^2 \right) + \frac{3}{8} f_+ \left(\beta - 1 + 2x \right)^2 + \frac{3}{8} f_- \left(\beta + 1 - 2x \right)^2 \right\}, \quad (3)$$

where x and β have been defined earlier.

Fig 3 shows the polarization fraction of the W against the c.m. energy. The principal effects occur in f_0 and f_- , especially when \sqrt{s} is close to m_V . The deviation at $\sqrt{s} = 500$ GeV is about 6% for parameter values of $b = 0.01$ and $g/g'' = 0.05$.

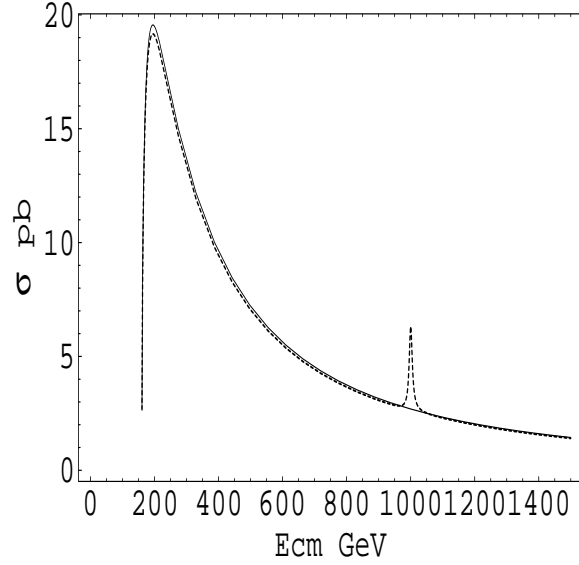


Figure 2: Cross section of $e^+e^- \rightarrow W^+W^-$ against c.m. energy. Solid curve shows the SM value, while the dashed one represents the BESS value. BESS parameters considered are $b = 0.01$, $g/g'' = 0.05$ and $m_V = 1$ TeV. Initial beams are unpolarised.

This is enhanced to a 25% effect at 800 GeV. Numerical values for the longitudinal W fraction, f_0 are given in Table 1 for $\sqrt{s} = 500$ GeV and 800 GeV. Lowering the value of g/g'' increases the sensitivity. This is because of the fact that the contributions proportional to b and g/g'' compensate each other in the range of parameters we are considering. Thus for example, with $b = 0.01$ and $g/g'' = 0.01$ deviation of f_0 is about 12% at 500 GeV, which goes up to about 54% at 800 GeV.

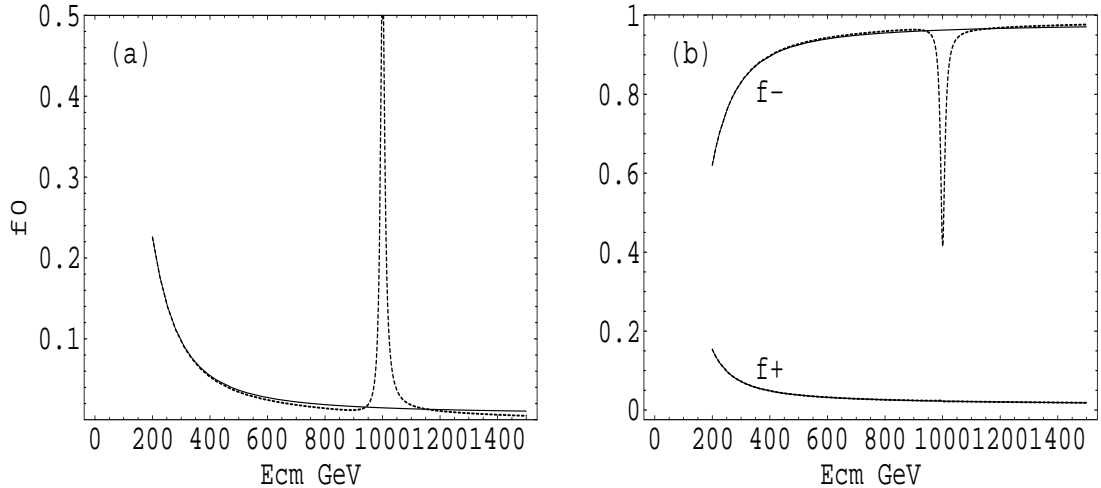


Figure 3: Fractional cross sections of (a) longitudinal W^- and (b) transverse W^- against c.m. energy. Solid curve shows SM value and dashed curve represents BESS value with parameters $b = 0.01$, $g/g'' = 0.05$ and $m_V = 1$ TeV. Unpolarised initial beams are considered.

We have also considered the case of polarized e^- beams. A priori, one would have thought that right-handed electron beam would have helped, as there is no neutrino exchange contribution in this case. On the contrary, it turns out that a left-handed

					$\sqrt{s} = 500 \text{ GeV}$		$\sqrt{s} = 800 \text{ GeV}$	
					$\sigma^{\text{BESS}}/\sigma^{\text{SM}}$	$f_0^{\text{BESS}}/f_0^{\text{SM}}$	$\sigma^{\text{BESS}}/\sigma^{\text{SM}}$	$f_0^{\text{BESS}}/f_0^{\text{SM}}$
$m_V = 1 \text{ TeV}$	0	0	0	0.05	1.003	1.075	1.012	1.597
			0.01	0.05	0.977	0.937	0.975	0.754
			0	0.01	1.000	1.003	1.000	1.021
			0.01	0.01	0.975	0.875	0.969	0.463
	-1	0	0	0.05	1.003	1.075	1.011	1.598
			0.01	0.05	0.977	0.921	0.973	0.625
			0	0.01	1.000	1.003	1.000	1.021
			0.01	0.01	0.975	0.859	0.969	0.379
$m_V = 2 \text{ TeV}$	0	0	0	0.05	1.002	1.061	1.005	1.253
			0.01	0.05	0.977	0.940	0.976	0.786
			0	0.01	1.000	1.002	1.000	1.009
			0.01	0.01	0.975	0.888	0.973	0.620
	-1	0	0	0.05	1.002	1.063	1.004	1.267
			0.01	0.05	0.977	0.927	0.975	0.728
			0	0.01	1.000	1.002	1.000	1.010
			0.01	0.01	0.973	0.620	0.973	0.561

Table 1: Ratios (BESS/SM) of total cross section and longitudinal fractions for different parameter values, without and with beam polarization. ($P_{e^-} = -1$ denotes left-handed electron polarization.)

electron beam is advantageous. This is because the new vector boson couples to the left-handed electrons much more strongly than to the right-handed ones. For example, with a left-handed electron beam and an unpolarised positron beam, deviation of f_0 is larger than in the case of unpolarised beams. At 800 GeV the deviation is improved from 25% with unpolarized beams to about 37% with left-polarized electron beam for a parameter set, $b = 0.01$ and $g/g'' = 0.05$. The corresponding improvement at 500 GeV is from 6% to 8%.

Table 1 shows that differences between BESS and SM remain detectable even if m_V is raised from 1 to 2 TeV. In particular the effect on f_0 is visible at 800 GeV for some parameter values, even with a resonance at 2 TeV.

3.3 Angular Spectrum of the Secondary Lepton:

We obtain the $\cos\theta_l$ distribution by integrating out x in Eq. 1. The result is shown in Fig. 4. The main effect is in the fraction of leptons at backward angles. At 500 GeV, only 3 to 4% of the decay leptons are in the backward-hemisphere ($\cos\theta_l < 0$). This fraction changes only by about 4 to 6% in going from SM to BESS. At 800 GeV the deviation becomes more significant ($\sim 21\%$). These results are summarised in Table 2.

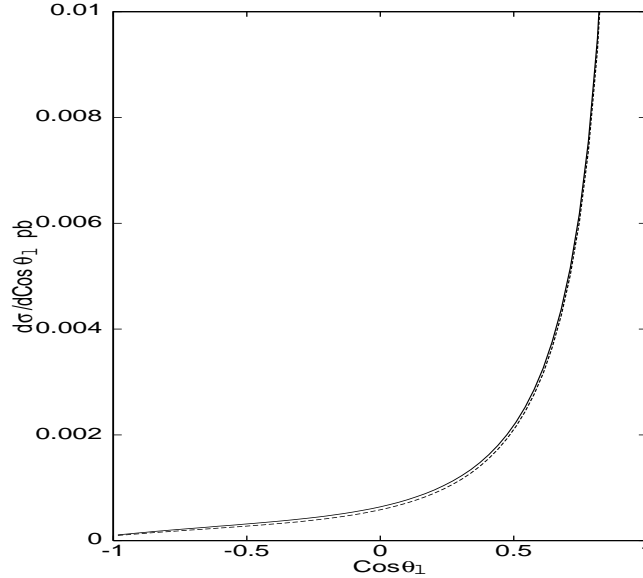


Figure 4: Lepton angular distribution in the case of BESS (dotted line) and SM (solid curve). BESS parameters are taken to be $b = 0.01$, $g/g'' = 0.05$ and $m_V = 1$ TeV. Beams are unpolarized and a c.m. energy of 800 GeV is considered. (Leptonic branching ratio not included.)

3.4 Energy-Angle Correlation:

Correlation in the case of the SM, $\frac{d\sigma^{\text{SM}}}{dE_l d\cos\theta_l}$ is plotted in Fig.5 (a), while Fig.5 (b) shows $(\frac{d\sigma^{\text{BESS}}}{dE_l d\cos\theta_l} - \frac{d\sigma^{\text{SM}}}{dE_l d\cos\theta_l})/(\frac{d\sigma^{\text{SM}}}{dE_l d\cos\theta_l})$. At a c.m. energy of 800 GeV maximum deviation is about 25% for a 1 TeV resonance with $b = 0.01$ and $g/g'' = 0.05$. Corresponding value at 500 GeV is about 8%. However, the larger deviations tend to occur in kinematic regions where the rate is small.

One practical application of the expression in Eq. 1 is that it allows us to calculate the effects of a geometrical cut that is imposed by limited detector acceptance. Such an angular cut results in a distortion of the observed energy distribution, as shown in Fig. 6.

3.5 High Energy Behaviour:

One of the generic features of a strongly interacting Higgs sector is that at sufficiently high energies, the longitudinal W fraction dominates. We have checked this by looking

					$\sqrt{s} = 500 \text{ GeV}$		$\sqrt{s} = 800 \text{ GeV}$	
					$\sigma \text{ pb}$	f_{back}	$\sigma \text{ pb}$	f_{back}
$m_V = 1 \text{ TeV}$	0	0	S.M.		7.144	0.034	3.713	0.024
			0	0.05	7.165	0.036	3.758	0.029
			0.01	0.05	6.981	0.033	3.620	0.022
			0	0.01	7.144	0.034	3.715	0.024
			0.01	0.01	6.964	0.032	3.600	0.019
	-1	0	S.M.		14.231	0.032	7.407	0.022
			0	0.05	14.269	0.033	7.486	0.027
			0.01	0.05	13.901	0.031	7.210	0.019
			0	0.01	14.232	0.032	7.410	0.023
			0.01	0.01	13.871	0.030	7.180	0.017
$m_V = 2 \text{ TeV}$	0	0	S.M.		7.144	0.034	3.713	0.024
			0	0.05	7.160	0.036	3.731	0.026
			0.01	0.05	6.982	0.033	3.622	0.022
			0	0.01	7.144	0.034	3.714	0.024
			0.01	0.01	6.968	0.032	3.611	0.020
	-1	0	S.M.		14.231	0.032	7.407	0.022
			0	0.05	14.261	0.033	7.441	0.025
			0.01	0.05	13.904	0.031	7.223	0.020
			0	0.01	14.232	0.032	7.409	0.022
			0.01	0.01	13.879	0.030	7.204	0.019

Table 2: Total WW cross section and backward fraction in the SM and BESS model for different parameter values. (Leptonic branching ratio not included in σ .)

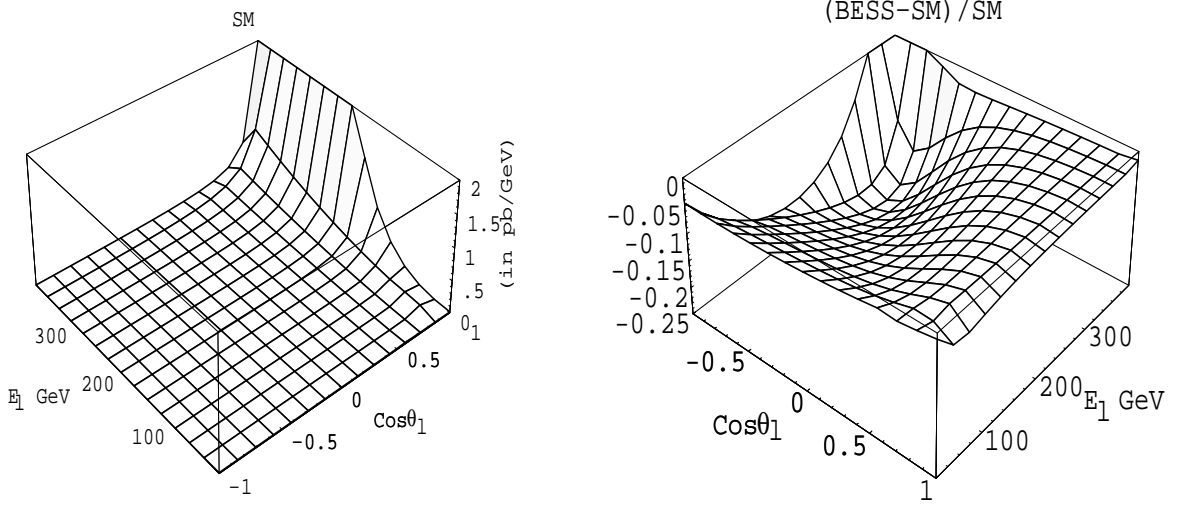


Figure 5: (a) Correlation of leptonic energy and polar angle in the lab frame in the case of SM. (b) Difference of the correlations in the BESS model and the SM. BESS parameters used are $b = 0.01$, $g/g'' = 0.05$ and $m_V = 1$ TeV. Initial beams are unpolarised and a c.m. energy of 800 GeV is considered in both the cases. (Leptonic branching ratio not included.)

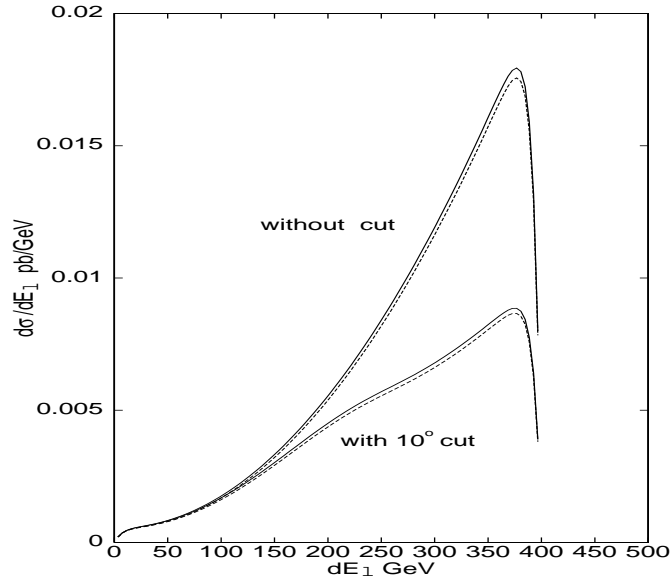


Figure 6: Lepton energy distribution in the case of BESS (dotted lines) and SM (solid curves). Upper set of curves is without any angular cut, while the lower set is with a cut $170^\circ \leq \theta_l \leq 10^\circ$ on the polar angle of the lepton. BESS parameters are taken to be $b = 0.01$, $g/g'' = 0.05$ and $m_V = 1$ TeV. Beams are unpolarized and a c.m. energy of 800 GeV is considered. (Leptonic branching ratio not included.)

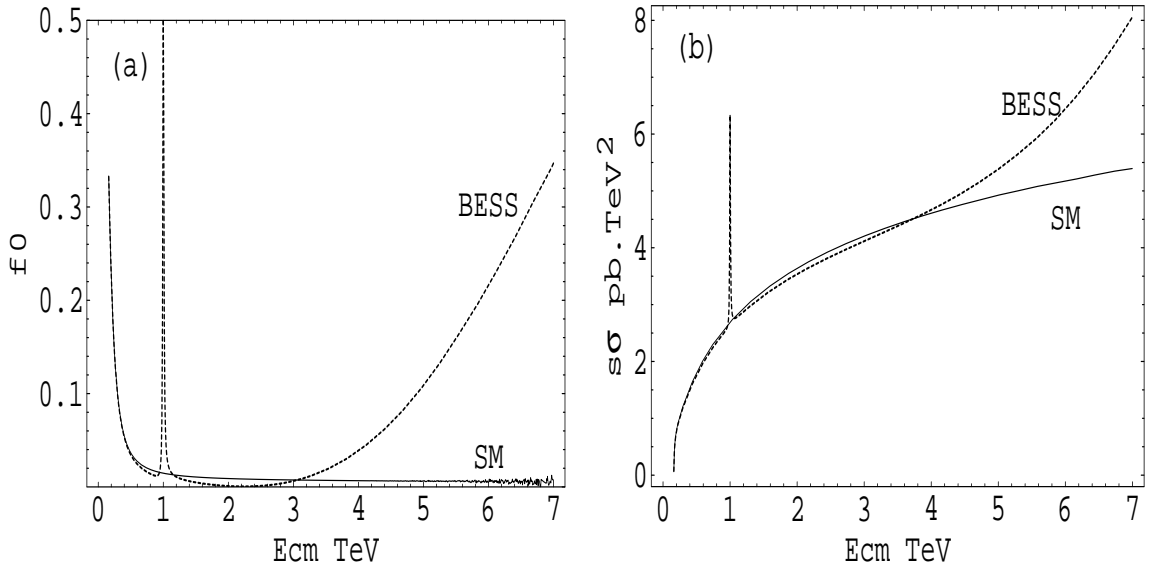


Figure 7: (a) f_0 and (b) $s\sigma$ against c.m. energy in the case of SM and BESS with parameters $b = 0.01$, $g/g'' = 0.05$ and $m_V = 1$ TeV. Unpolarized beams are considered.

at the behaviour of $f_0(\sqrt{s})$ at energies far above the resonance. As seen from Fig. 7(a), the expected dominance of f_0 sets in at multi-TeV energies. Likewise, one expects that in the BESS model (as contrasted with the SM) the cross section $\sigma(e^+e^- \rightarrow W^+W^-)$ will deviate from the $\frac{1}{s}$ behaviour, and ultimately become divergent, violating the unitarity limit, $\sigma < 12\pi/s$. This behaviour is also confirmed, as shown in Fig. 7(b). The features shown in Fig. 7 are symptomatic of any non-standard model with a strongly interacting Higgs sector.

4 Summary

We have studied the secondary lepton spectra coming from the WW pairs produced in e^+e^- collisions to see the effect of the BESS model relative to the SM. Our studies are complementary to earlier studies done on $e^+e^- \rightarrow W^+W^-$ which focussed on primary observables.

With parameters allowed by low energy constraints from LEP and SLC we find that a BESS type resonance in the 1 to 2 TeV region can produce small effects in observables measured at e^+e^- energies of $\sqrt{s} = 500$ to 800 GeV. These effects occur, in particular, in the longitudinal helicity fraction f_0 , which may be obtained from the energy spectrum of the secondary lepton (see Eq. 3). They also appear in the fraction of secondary leptons produced in the backward hemisphere. A typical effect is a change in the value of f_0 from 3% in SM to 4% in BESS. Information on lepton spectra can eventually be incorporated in an analysis such as that performed in Ref. [8] in order to delineate the parameter space $(g/g'', b)$ of the BESS model.

Acknowledgements

One of us, P.P. wishes to thank the Humboldt Foundation for a Post-doctoral Fellowship, and the Institute of Theoretical Physics, RWTH Aachen for the hospitality provided during this work. L.M.S. would like to acknowledge a Visiting Scientist award

from ICTP, Trieste, enabling visits to the Physical Research Laboratory, Ahmedabad, where this project was initiated.

Appendix

The coefficients, C 's in Eqn 1 are given by

$$\begin{aligned}
C_s &= g_{\gamma WW}^2 (c_\gamma^{v2} + c_\gamma^{a2}) + s_Z^2 g_{ZWW}^2 (c_Z^{v2} + c_Z^{a2}) + s_{V^2} g_{VWW}^2 (c_V^{v2} + c_V^{a2}) \\
&\quad + 2 s_Z g_{\gamma WW} g_{ZWW} (c_\gamma^v c_Z^v + c_\gamma^a c_Z^a) + 2 s_V g_{\gamma WW} g_{VWW} (c_\gamma^v c_V^v + c_\gamma^a c_V^a) \\
&\quad + 2 s_Z s_V g_{ZWW} g_{VWW} (c_Z^v c_V^v + c_Z^a c_V^a), \\
C'_s &= 2 (g_{\gamma WW}^2 c_\gamma^v c_\gamma^a + s_Z^2 g_{ZWW}^2 c_Z^v c_Z^a + s_{V^2} g_{VWW}^2 c_V^v c_V^a) \\
&\quad + s_Z g_{\gamma WW} g_{ZWW} (c_\gamma^v c_Z^a + c_\gamma^a c_Z^v) + s_V g_{\gamma WW} g_{VWW} (c_\gamma^v c_V^a + c_\gamma^a c_V^v) \\
&\quad + s_Z s_V g_{ZWW} g_{VWW} (c_Z^v c_V^a + c_Z^a c_V^v), \\
C_{int} &= g_{e\nu W}^2 (g_{\gamma WW} (c_\gamma^v - c_\gamma^a) + s_Z g_{ZWW} (c_Z^v - c_Z^a) + s_V g_{VWW} (c_V^v - c_V^a)), \\
C_t &= \frac{g_{e\nu W}^4}{2},
\end{aligned}$$

where the gauge couplings are given by

$$\begin{aligned}
g_{\gamma WW} &= 1, \\
g_{ZWW} &= \frac{\cos^2 \phi}{\tan \theta_W} \left(\frac{\cos \xi}{\cos \psi} + \tan \theta_W \tan \psi \sin \xi \right), \\
g_{VWW} &= \frac{\cos^2 \phi}{\tan \theta_W} \left(\frac{\sin \xi}{\cos \psi} - \tan \theta_W \tan \psi \cos \xi \right) + \frac{\cos \xi \sin^2 \phi}{2 \sin \theta_W} \frac{g''}{g}
\end{aligned}$$

and the fermionic couplings by

$$\begin{aligned}
g_{e\nu W} &= -\frac{1}{\sqrt{2x_W} (1+b)} \left(\frac{\cos \phi}{\cos \psi} - \frac{b}{2} \frac{g}{g''} \frac{\sin \phi}{\cos \psi} \right), \\
c_\gamma^v &= 1, & c_\gamma^a &= 0, \\
c_Z^v &= -\frac{1}{4 \sin \theta_W \cos \theta_W} (-A + 4 B), & c_Z^a &= \frac{A}{4 \sin \theta_W \cos \theta_W}, \\
c_V^v &= -\frac{1}{4 \sin \theta_W \cos \theta_W} (-C + 4 D), & c_V^a &= \frac{C}{4 \sin \theta_W \cos \theta_W}
\end{aligned}$$

with

$$\begin{aligned}
A &= \frac{\cos \xi}{\cos \psi (1+b)} \left(1 + b \sin^2 \theta_W \left(1 - \frac{\tan \xi}{\tan \theta_W \sin \psi} \right) \right), \\
B &= \frac{\cos \xi}{\cos \psi} \left(1 - \frac{\tan \xi}{\tan \theta_W \sin \psi} \right) \sin^2 \theta_W, \\
C &= \frac{\sin \xi}{\cos \psi (1+b)} \left(1 + b \sin^2 \theta_W \left(1 + \frac{\cot \xi}{\tan \theta_W \sin \psi} \right) \right), \\
D &= \frac{\sin \xi}{\cos \psi} \left(1 + \frac{\cot \xi}{\tan \theta_W \sin \psi} \right) \sin^2 \theta_W.
\end{aligned}$$

Here ϕ , ξ and ψ are functions of BESS parameters as given below.

$$\phi = -\frac{g}{g''}, \quad \xi = -\frac{\cos 2\theta_W}{\cos \theta_W} \frac{g}{g''} \quad \text{and} \quad \psi = 2 \sin \theta_W \frac{g}{g''},$$

where g is the standard electroweak coupling. The propagator factors are

$$s_Z = \frac{s}{s - m_Z^2}, \quad s_V = \frac{s(s - m_V^2)}{(s - m_V^2)^2 + \Gamma_V^2 m_V^2} \quad \text{and} \quad s_{V^2} = \frac{s^2}{(s - m_V^2)^2 + \Gamma_V^2 m_V^2}.$$

References

- [1] M. Veltman, *CERN-97-05* and references therein.
- [2] R. Casalbuoni, S. De Curtis, D. Dominici, R. Gatto, *Phys. Lett.* **B 155** (1985) 95; *Nucl. Phys.* **B 282** (1987) 235; R. Casalbuoni, A. Deandrea, S. De Curtis, D. Dominici, R. Gatto, *hep-ph/9708287*, T.L. Barklow, G. Burdman, R. S. Chivukula, B.A. Dobrescu, P.S. Drell, N. Hadley, W.B. Kilgore, M. E. Peskin, J. Terning, D.R. Wood, *hep-ph/9704217*; R.D. Heuer, D. Miller, F. Richard, P. Zerwas, *TESLA Technical Design Report: Part III*, DESY-2001-011 (*hep-ph/0106315*).
- [3] A. P. Balachandran, A. Stern, G. Trahern, *Phys. Rev.* **D 19** (1979) 2416.
- [4] M. Bando, T. Kugo, K. Yamawaki, *Phys. Rep.* **164** (1988) 217.
- [5] G. Altarelli and R. Barbieri, *Phys. Lett.* **B 253** (1991) 161; G. Altarelli, R. Barbieri and S. Jadach, *Nucl. Phys.* **B 369** (1992) 3.
- [6] R. Casalbuoni, S. De Curtis, D. Guetta, *hep-ph/9912377*.
- [7] LEP Collaborations, *LEPEWWG/XSEC/2001-03*.
- [8] R. Casalbuoni, P. Chiappetta, A. Deandrea, S. De Curtis, D. Dominici, R. Gatto, *Z. Phys.* **C 60** (1993) 315.
- [9] V.A. Koval'chuk, M.P. Rekalov, I.V. Stoletnii, *Z. Phys.* **C 23** (1984) 111.
- [10] L3 Collaboration, *Phys. Lett.* **B 74** (2000) 194; L3 Note 2636
- [11] A. Werthenback, L.M. Sehgal, *Phys. Lett.*, **B 402** (1997) 189.
- [12] D.A. Dicus and K. Kallianpur, *Phys. Rev.* **D 32** (1985) 35.